Lattice Parameters and Site Occupancy Factors of Magnetite-Maghemite Core-Shell Nanoparticles. A Critical Study.

Antonio Cervellino[a], Ruggero Frison[b], Giuseppe Cernuto[c], Antonietta Guagliardi[b,c]* and Norberto Masciocchi[c]

[a] Swiss Light Source, Paul Scherrer Institut, 5232, Villigen, Switzerland

[b]Istituto di Cristallografia and To.Sca.Lab, National Council of Research, via Lucini, 3, Como, 22100, Italy

[c]Dipartimento di Scienza e Alta Tecnologia and To.Sca.Lab, Università dell'Insubria, via Valleggio, 11, Como, 22100, Italy

Correspondence email: antonella.guagliardi@ic.cnr.it

Supporting Information

Table S1 Synoptic collection of all investigated samples: synthesis conditions, post-synthesis treatment [in the (1) and (2) sequence], DFA most relevant results.

Sample	Synthesis Conditions[1]		Post-Synthesis (1)	Post-Synthesis (2)	Debye Function Analysis Results			
	[M] Fe(II)	*[M] Fe(III)*	*Temp. (°C), Time (h),*	*Temp. (°C), Time (h),*	$<D>_M$ [nm]	σ_M [nm]	$<Cell>_M$ (err) [Å]	<3-δ> (err)
A1	0.017	0.034	50, 16, a[2]		8.54	3.75	8.363(2)	2.76(1)
A2	0.050	0.100	50, 16, a		10.06	4.93	8.363(1)	2.78(1)
A3	0.050	0.100	r.t., 16, a		9.44	4.02	8.376(1)	2.86(1)
A4	0.050	0.100	50, 16, v[2]		9.52	3.91	8.373(1)	2.85(1)
A5	0.100	0.200	50, 16, a		10.59	3.99	8.366(1)	2.79(2)
A6	0.100	0.200	50, 16, a	r.t., 2, H_2O_2	10.52	3.98	8.365(1)	2.77(1)
A7	0.100	0.200	50, 16, a	200, 3, a	10.43	4.48	8.349(1)	2.694(4)
A8	0.100	0.200	50, 16, a	200, 16, a	10.70	4.14	8.347(1)	2.677(9)
B1	0.005	0.010	r.t., 2, v		8.99	3.03	8.356(2)	2.725(4)
B2	0.050	0.100	r.t., 2, v		9.92	3.57	8.357(2)	2.71(1)
B3	0.100	0.200	r.t., 2, v		10.12	3.88	8.359(1)	2.75(1)
B4	0.250	0.500	r.t., 2, v		9.61	3.68	8.361(2)	2.72(1)
B5	0.250	0.500	r.t., 2, v	50, 6, a	9.54	3.88	8.360(1)	2.72(1)
B6	0.250	0.500	r.t., 2, v	100, 6, a	9.63	3.85	8.354(2)	2.702(5)
B7	0.250	0.500	r.t., 2, v	150, 6, a	9.83	3.72	8.351(2)	2.68(1)
B8	0.250	0.500	r.t., 2, v	200, 6, a	9.66	4.10	8.349(1)	2.675(4)
B9	0.250	0.500	r.t., 2, v		10.00	3.97	8.372(3)	2.826(8)
C1	0.365	0.333	r.t., 16, a		12.76	6.32	8.383(1)	2.953(4)
C2	0.050	0.000	r.t., 16, a		27.77	14.29	8.396(1)	2.988(6)
C3	0.050	0.000	r.t., 16, a		20.20	9.85	8.386(1)	2.90(2)
C4	0.100	0.000	50, 3, a		18.48	9.22	8.3758(8)	2.89(2)
C5	0.050	0.000	r.t., 16, a		23.84	11.37	8.3870(9)	2.92(2)
C6	0.050	0.000	r.t., 16, a	100, 1, a	25.25	11.64	8.364(1)	2.83(1)
C7	0.050	0.000	r.t., 16, a	150, 2, a	28.55	14.14	8.3481(6)	2.70(4)
D1	0.050	0.100	50, 16, a		10.05	4.10	8.358(1)	2.76(1)
D2	0.050	0.100	50, 16, a		9.68	4.13	8.358(2)	2.72(2)
D3	0.050	0.100	50, 16, a		9.37	4.51	8.357(1)	2.74(2)
E1	0.050	0.100	r.t., 16, a		8.77	4.62	8.369(2)	2.81(2)
F1	0.400	0.800	r.t., 2, v		8.25	3.60	8.361(2)	2.72(2)
G1	--	0.100	50, 16, a		-	-	-	-

(1) Solvent: H_2O (A, B, C, G groups); H_2O:EtOH 3:1 (D group); H_2O/CTAB/ 1-Butanol/1-Octanol (E1); HCl 0.5 M (F1). Base: NH_3 (A, B, C, D, E, G groups); NaOH (F1).

(2) a = air, v = vacuum

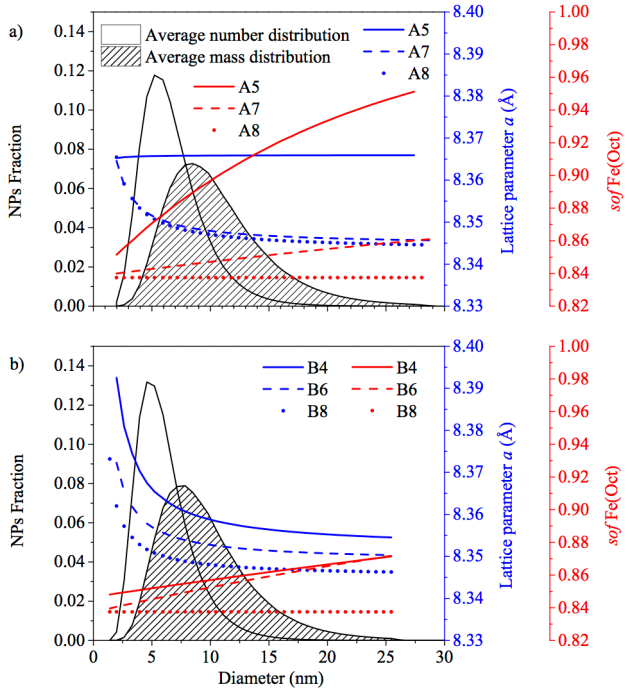

Figure S1 Number- and mass-based size distributions (solid black curve and dashed area, respectively) for: (a) the sample A5 and after heating it at 200 °C in air for 3 h (A7) and 16 h (A8), and for: (b) the sample B4 and after heating it in air for 6h at 100°C (B6) and 200°C (B8). Blue (continuous, dashed and dotted) lines depict the size-dependent behavior of the cell parameter in the pristine sample and upon the oxidative thermal treatment, affecting the *sof* of Fe(Oct) according to the (continuous, dashed and dotted) red curves. The initial lattice parameter (nearly constant throughout all the sizes in A5 and showing a large inflation below 5 nm in B4) turns into a lattice contraction due to the oxidation in which the smallest NPs, although more oxidized, show larger lattice parameters than the largest NPs.

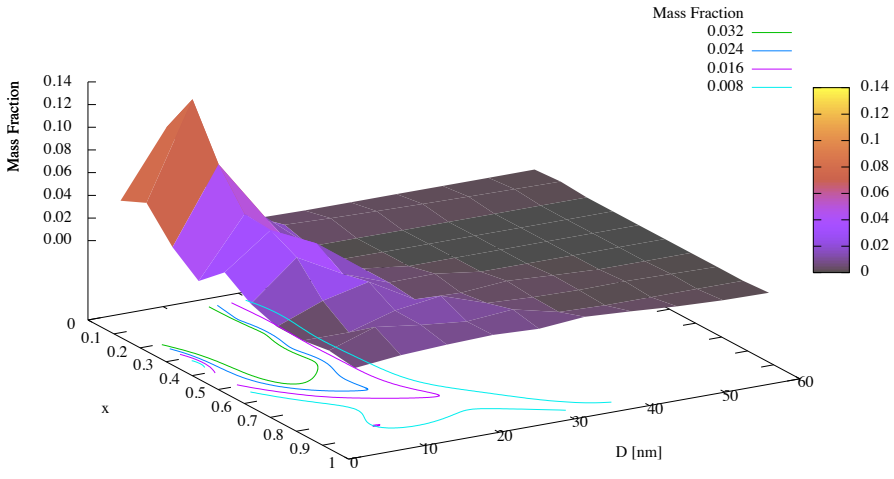

Figure S2. 3D map describing the average mass fraction (over all samples, i.e. the mass fractions in each sample divided by the number of samples) of the NPs as a function of size (*D*) and stoichiometry (*x*). Points have been binned in a 10x10 square grid with bin sizes of 6 nm for *D* and 0.1 for *x*. In each bin the mass fractions of NPs from any sample having D and x within the bin boundary have been summed. As the mass fraction is proportional to the relative full-pattern integrated intensity, this is a measure of significance of each bin within this study. In fact, a completely similar plot can be obtained using, instead of the mass fractions, the statistical weights (the inverse square standard deviations) of the relevant NPs lattice parameter or stoichiometry parameter *x* (see fig. S1).